A Surprising Role for the Sch9 Protein Kinase in Chromosome Segregation in *Candida albicans*

Neha Varshney,*,[1] Alida Schaekel,[†,‡,1] Rima Singha,* Tanmoy Chakraborty,*,[2] Lasse van Wijlick,[†,‡] Joachim F. Ernst,[†,‡,3] and Kaustuv Sanyal*,[3]

*Molecular Mycology Laboratory, Jawaharlal Nehru Centre for Advanced Scientific Research, Jakkur, Bangalore 560064, India, and [†]Department Biologie, Molekulare Mykologie and [‡]Manchot Graduate School Molecules of Infection, Heinrich-Heine-Universität, Düsseldorf 40225, Germany

ORCID ID: 0000-0002-6611-4073 (K.S).

ABSTRACT The AGC kinase Sch9 regulates filamentation in *Candida albicans*. Here, we show that Sch9 binding is most enriched at the centromeres in *C. albicans*, but not in *Saccharomyces cerevisiae*. Deletion of CaSch9 leads to a 150- to 750-fold increase in chromosome loss. Thus, we report a previously unknown role of Sch9 in chromosome segregation.

KEYWORDS kinase, Sch9, centromere, chromosome segregation, kinetochore

TARGET of rapamycin complex 1 (TORC1) is a major regulator of cell growth and a nutrient sensor in all eukaryotic cells. In the pathogenic yeast *Candida albicans*, the AGC kinase Sch9, one of the direct downstream targets of TORC1, represses filamentation in hypoxia and under high CO_2 conditions. Sch9 performs distinct functions in growth and morphogenesis depending on the availability of O_2 and CO_2 (Stichternoth *et al.* 2011). Earlier studies indicated that absence of Sch9 increases the chronological life span of *Saccharomyces cerevisiae* (Fabrizio *et al.* 2001). However, *sch9* mutant cells of *C. albicans* have a reduced longevity only under normoxic conditions and not under hypoxic conditions (Stichternoth *et al.* 2011).

In this study, we sought to determine the genomic binding sites of the HA-tagged Sch9 protein by ChIP on chip (ChIP-chip) experiments under normoxia as well as hypoxia with and without elevated CO_2 levels in *C. albicans*. Remarkably, the major binding peaks of Sch9 coincided with the centromere (*CEN*) regions. Centromeric Sch9 binding was observed under normoxia (Figure 1A) as well as under hypoxia with or without 6% CO_2 (Figure 1B). Under all conditions, a few reproducible Sch9 binding peaks occurred outside the *CEN* regions as well (not shown). The ChIP-chip data were validated by semiquantitative (data not shown) and quantitative PCR (qPCR) analysis using *CEN5*- and *CEN7*-specific primers (Figure 1C).

Enrichment of Sch9 binding at *CEN* regions led us to examine its possible role in the stability of the kinetochore, a multiprotein complex formed on the *CEN* DNA. The centromere–kinetochore complex plays a central role in the microtubule–kinetochore-mediated process of chromosome segregation. First, we analyzed the nuclear morphology in wild-type (CAI4) and mutant cells (CAS1 and CCS3) (strain construction, Southern confirmation, and genotype of strains are described in the Supporting Information, File S1, Figure S1 and Table S1, respectively). Except for a marginal increase in proportion of large-budded cells (at G2/M stage) with the unsegregated nucleus in the *sch9* mutant cells (CAS1 and CCS3) as compared to the wild type (CAI4), no significant difference was evident (Figure S2). A marginal increase observed in the proportion of large-budded mutant cells having an unsegregated nuclear mass as compared to wild type is insignificant, since the wild-type cells also showed unsegregated DNA mass, as expected, during the pre-anaphase stage of the cell cycle. Moreover, a significant delay in G1 in the *sch9* mutant added to the complexity of analysis. Like *S. cerevisiae*, centromeres are clustered

doi: 10.1534/genetics.114.173542
Manuscript received December 11, 2014; accepted for publication January 6, 2015; published Early Online January 15, 2015.
Supporting information is available online at http://www.genetics.org/lookup/suppl/doi:10.1534/genetics.114.173542/-/DC1.
ChIP-chip data have been deposited at http://www.candidagenome.org/download/systematic_results/Chakraborty_2014/.
[1]These authors contributed equally to this work.
[2]Present address: Department of Microbiology, University of Szeged, Kőze´pfasor, Szeged, Hungary 672.
[3]Corresponding authors: Department Biologie, Molekulare Mykologie, Heinrich-Heine-Universität Düsseldorf, Universitätsstr.1/Geb. 26.12, 40225 Düsseldorf, Germany. E-mail: joachim.ernst@uni-duesseldorf.de; Molecular Mycology Laboratory, Molecular Biology and Genetics Unit, Jawaharlal Nehru Centre for Advanced Scientific Research, Jakkur, Bangalore 560064, India. E-mail: sanyal@jncasr.ac.in

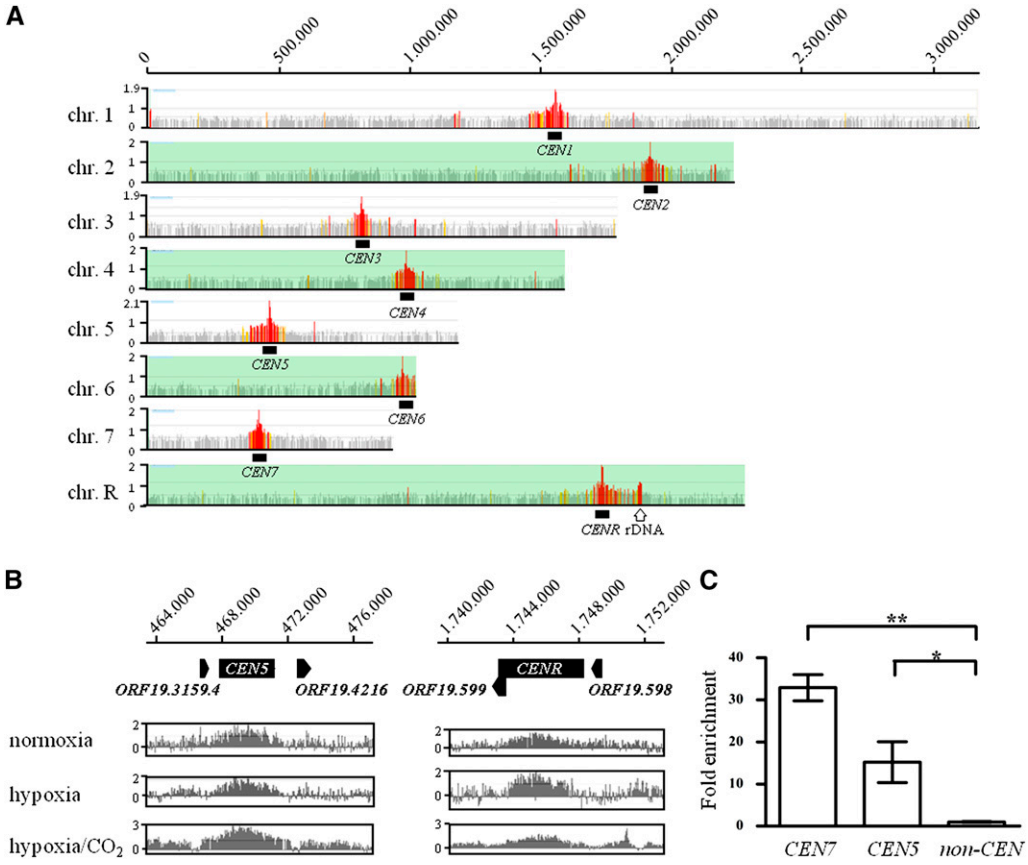

Figure 1 Genomic localization of the Sch9 kinase. The ChIP-chip procedure was carried out essentially as described previously (Lassak *et al.* 2011; Schaekel *et al.* 2013). *C. albicans* genomic tiling microarrays (NimbleGen) were probed pair-wise by immunoprecipitated chromatin of a strain expressing HA-tagged Sch9 (AF1006) and the corresponding control strain (CAS1). Two independent cultures were assayed for each combination of strains. (A) An overview of Sch9 binding. Significant binding peaks were calculated by the NimbleScan software (NimbleGen) and color-coded according to their FDR values in red [false discovery rate (FDR) ≤ 0.05], orange (FDR ≤ 0.1), yellow (FDR 0.1–0.2), and gray (FDR > 0.2). Significant Sch9-binding peaks were detected at centromeres by genomic ChIP-chip on all *C. albicans* chromosomes. In addition, a significant peak occurred at the rDNA locus (open arrow). (B) Examples for centromeric binding of Sch9 at *CEN5* and *CENR*. Scaled $\log_2$ ratios of cells grown in normoxia and hypoxia with or without 6% CO_2 are shown. Note that Sch9 enrichment was obtained for cells grown under normoxia or hypoxia conditions. (C) Enrichment at *CEN7*, *CEN5*, and the noncentromeric region was analyzed using qPCR. qPCR analysis reveals the mean fold enrichment of Sch9 at the centromeres obtained in two independent ChIP experiments (±SD) relative to the no-tag control and normalized to the input samples. The calculation was done with two biological replicates (two ChIP samples), and each measurement was performed in triplicate. Significant difference was observed in Sch9 recruitment at the *CEN5* and *CEN7* region ($P < 0.05$) and ($P < 0.01$), respectively (shown by asterisks).

throughout the cell cycle in *C. albicans* (Roy *et al.* 2011; Sanyal and Carbon 2002; Thakur and Sanyal 2012). Depletion of an essential kinetochore protein leads to centromere declustering and delocalization of the centromere-specific histone Cse4 in *C. albicans* (Thakur and Sanyal 2012). However, we found neither centromere declustering nor any significant change in the centromeric histone Cse4 levels at the kinetochore (Cse4-GFP intensity) in wild-type (strain 8675) and *sch9* mutant (strain 8675T) strains (Figure 2A). To further investigate the role of Sch9 in Cse4 localization at the centromeres, we performed Cse4-ChIP assays with wild-type (J200) and mutant cells (J200T). We analyzed enrichment of Cse4 at *CEN5* and *CEN7* regions both by semiquantitative (Figure S3) and qPCR (Figure 2B) (primer sequences are listed in Table S2). Cse4 binding was found to be similar at the centromeres in the presence or absence of Sch9. Thus, Sch9 does not seem to play a direct role in Cse4-mediated kinetochore integrity in *C. albicans*.

Many kinetochore proteins play crucial but nonessential roles in the process of chromosome segregation (Sanyal *et al.* 1998; Ortiz *et al.* 1999; Poddar *et al.* 1999; Ghosh *et al.* 2001; Measday *et al.* 2002). The centromeric localization of Sch9 prompted us to examine whether Sch9 plays a role in high-fidelity chromosome segregation. One or both of the alleles of *SCH9* were deleted from the diploid genome of the *C. albicans* wild-type strain RM1000AH, which was previously used to study chromosome loss (Sanyal *et al.* 2004). Each homolog of chromosome 7 is marked by the auxotrophic marker *HIS1* or *ARG4* in RM1000AH (Figure 3A). The strains were confirmed by Southern blot analysis (Figure S1). We previously reported that the natural rate of loss of a chromosome in wild-type *C. albicans* (SN148) is $<5 \times 10^{-4}$/cell/generation (Mitra *et al.* 2014). Two independent null (*sch9/sch9*) mutant strains (RMKS2A and RMKS2B) exhibited a 150- to 750-fold increase in chromosome loss as compared to the spontaneous rate of loss of a chromosome (Figure 3B). Even heterozygous (*SCH9/sch9*) mutants of *SCH9* (RMKS1A and RMKS1B) exihibited chromosome loss at a rate higher than the wild type (Figure 3B). This high rate of chromosome loss is comparable to the loss rate exhibited by several *S. cerevisiae* kinetochore mutants. The role of Sch9 in chromosome segregation was further validated by re-integrating the *SCH9* ORF, including its native promoter and terminator sequences at the *RPS10* locus. While the chromosome loss was completely suppressed in re-integrants (RMKS1AR and RMKS1BR) generated in the *SCH9/sch9* mutant background (RMKS1A and RMKS1B), a reduced rate of loss was observed in re-integrants (RMKS2AR and RMKS2BR) in the *sch9/sch9* null mutant background (RMKS2A and RMKS2B) (Figure 3C). While this assay measures the loss of

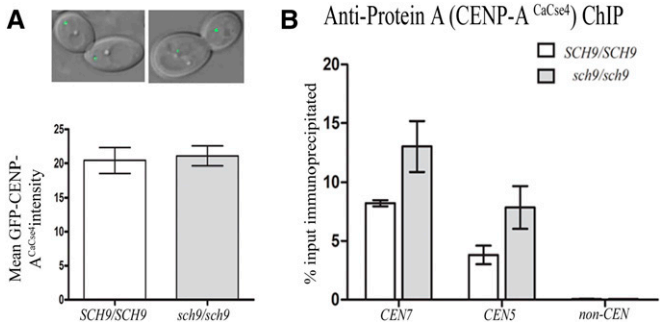

Figure 2 Sch9 is not required for Cse4-mediated kinetochore stability. (A) Microscopy images showing Cse4-GFP signal intensities in wild-type 8675 (*CSE4-GFP/CSE4;SCH9/SCH9*) and mutant 8675T (*CSE4-GFP/CSE4; sch9/sch9*). *C. albicans* wild-type and mutant strains where *CSE4* is GFP-tagged were grown overnight at 30° under normoxic conditions in YPDU (1% yeast extract, 2% peptone, 2% dextrose supplemented with 10mg/100ml uridine) and washed with water, and images were taken using a confocal laser-scanning microscope (LSM 510 META, Carl Zeiss). The brightest GFP signal in each cell was determined using the Image J software as described before (Roy *et al.* 2011). Briefly, an equal area from each cell was selected. The average pixel intensity was measured and corrected for the background by subtracting the lowest pixel intensity value in the field from the average. Then the mean GFP intensity was measured using the Image J software and the graph was plotted using Graph Pad Prism. Measurement was taken from 45 cells in each case. The experiment was performed twice. Standard error of mean (*t*-test) was used to calculate statistical significance ($P < 0.05$). For strain construction (see Supporting Information). (B) Cse4 localization at the centromere is not affected by absence of Sch9. Standard ChIP assays were performed on strains CAKS102 (*CSE4-TAP/CSE4;SCH9/SCH9*) and J200T (*CSE4-TAP/Cse4*; *sch9/sch9*) (grown at 30° under normoxic conditions) using anti-Protein A antibodies. Enrichment at *CEN7*, *CEN5*, and the noncentromeric region was analyzed by qPCR. PCR using total DNA (T) or ChIP DNA fractions with (+) or without (−) antibodies was performed. qPCR analysis revealed the enrichment of Cse4 at the centromere as a percentage of the total chromatin input, and values were plotted as mean of triplicates ±SD. No significant difference was observed in CaCse4 recruitment at the *CEN5* and *CEN7* region ($P > 0.05$). Percentage input was calculated as 100*2^[adjusted input − Ct(IP)] (Mukhopadhyay *et al.* 2008).

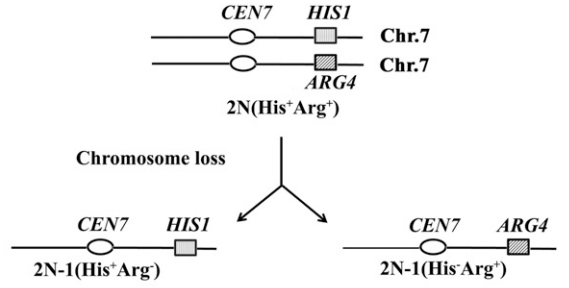

B

Strain name	Genotype	No. of colonies			Chromosome loss rate/ cell/generation
		YPDU	$His^+ Arg^-$	$His^- Arg^+$	
RM1000AH	*SCH9/SCH9*	995	0	0	$<1.0X10^{-3}$
RMKS1A	*SCH9/sch9*	725	3	1	$5.5X10^{-3}$
RMKS1B		1127	1	1	$1.8X10^{-3}$
RMKS2A	*sch9/sch9*	865	8	5	$15.0X10^{-3}$
RMKS2B		989	3	0	$3.0X10^{-3}$

C

Strain name	Genotype	No. of colonies			Chromosome loss rate/ cell/generation
		YPDU	$His^+ Arg^-$	$His^- Arg^+$	
RMKS1AR	*SCH9/sch9/ CIp10-SCH9*	942	0	0	$<1.0X10^{-3}$
RMKS1BR		964	0	0	$<1.0X10^{-3}$
RMKS2AR	*sch9/sch9/ CIp10-SCH9*	1102	6	0	$5.0X10^{-3}$
RMKS2BR		985	0	0	$<1.0X10^{-3}$

Figure 3 Chromosome loss assay. (A) Schematic of chromosome loss assay. (B and C) The chromosome loss assay was performed with two independent transformants of both mutants and revertants, as described before (Sanyal *et al.* 2004). The numbers indicate the summation of colonies patched in independent experiments. Briefly, the strains were grown for ~20 generations on YPDU medium at 30° under normoxic conditions. Subsequently, ~1000 cells were plated on YPDU agar plates for each transformant and incubated at 30° for 2 days. The single colonies were patched on YPDU, SD minimal medium (SD) without arginine (CM−arg), and SD without histidine (CM−his). The chromosome loss rate was calculated by the number of colonies that were unable to grow on selective media divided by the total number of colonies grown on nonselective media.

heterozygosity, the loss of an unlinked single nucleotide polymorphism (SNP) on chromosome 7 along with the loss of a marker gene on the same chromosome could determine the loss of the entire chromosome. We observed that SNPs on chromosome 7 in the strains used in this study are absent, as compared to another *C. albicans* strain reported previously (Forche *et al.* 2009). However, binding of Sch9 to all centromeres combined with a higher rate of loss of the marker gene by the homozygous and heterozygous mutants led us to conclude that absence of Sch9 indeed increases the rate of chromosome loss. This confirms the critical role of Sch9 in the high-fidelity process of chromosome segregation.

To verify if centromere DNA binding of the Sch9 kinase also occurs in other yeast species outside the *Candida*-specific CTG clade, we carried out a genome-wide ChIP-chip experiment to localize HA-tagged ScSch9 (Pascual-Ahuir and Proft 2007) in *S. cerevisiae*. No detectable binding of ScSch9 to any centromere region was found. However, as in *C. albicans*, the ribosomal DNA (rDNA) locus showed significant ScSch9 binding in *S. cerevisiae* (data not shown). We conclude that Sch9 binding to centromeres is not a general feature among Hemiascomycetes fungi and may have arisen specifically in *C. albicans*, a member of the CTG clade, while binding to rDNA remained conserved. It would be tempting to speculate that the association of Sch9 with centromeres might have arisen specifically in the CTG clade. Nevertheless, Sch9 is important for growth in both *S. cerevisiae* and *C. albicans* (Pascual-Ahuir and Proft 2007; Stichternoth *et al.* 2011).

Rapid fungal growth requires effective biosynthetic, metabolic, and regulatory activities of cells. Nutrient abundance is signaled by the Tor1 pathway via the Sch9 AGC kinase. Thus, the remarkable strong binding of Sch9 to centromeres could be related to effective chromosomal replication. Incidentally,

deletion of a centromere-proximal replication origin leads to a moderate increase in chromosome loss (Mitra *et al.* 2014). In addition, phospho-regulation of kinetochore proteins by kinases (such as Aurora B kinase/polo-like kinase 1) has been shown to be critical for proper chromosome segregation (Shang *et al.* 2003; McKinley and Cheeseman 2014). Unlike short 125-bp, genetically determined, sequence-specific point centromeres of *S. cerevisiae*, *C. albicans* chromosomes contain unique sequence-independent epigenetically specified regional centromeres (Sanyal *et al.* 2004; Baum *et al.* 2006; Thakur and Sanyal 2013). While the targets of this AGC kinase Sch9 are largely unknown, centromere binding of this protein selectively in *C. albicans* but not in *S. cerevisiae* provides new insights of functional evolution of a protein in organisms having different types of centromeres.

Acknowledgments

This work was supported by a grant from the Department of Biotechnology, Government of India, and intramural funding from the Jawaharlal Nehru Centre for Advanced Scientific Research (to K.S.) and by grants from the Jürgen Manchot Stiftung Düsseldorf (to A.S. and L.v.W.) and the ERA-NET PathoGenoMics project OXYstress (to J.F.E.). N.V. and R.S. are supported by fellowships from the Council of Scientific and Industrial Research and University Grants Commission (Government of India), respectively.

Literature Cited

Baum, M., K. Sanyal, P. K. Mishra, N. Thaler, and J. Carbon, 2006 Formation of functional centromeric chromatin is specified epigenetically in Candida albicans. Proc. Natl. Acad. Sci. USA 103: 14877–14882.

Fabrizio, P., F. Pozza, S. D. Pletcher, C. M. Gendron, and V. D. Longo, 2001 Regulation of longevity and stress resistance by Sch9 in yeast. Science 292: 288–290.

Forche, A., M. Steinbach, and J. Berman, 2009 Efficient and rapid identification of Candida albicans allelic status using SNP-RFLP. FEMS Yeast Res. 9: 1061–1069.

Ghosh, S. K., A. Poddar, S. Hajra, K. Sanyal, and P. Sinha, 2001 The IML3/MCM19 gene of Saccharomyces cerevisiae is required for a kinetochore-related process during chromosome segregation. Mol. Genet. Genomics 265: 249–257.

Lassak, T., E. Schneider, M. Bussmann, D. Kurtz, J. R. Manak *et al.*, 2011 Target specificity of the Candida albicans Efg1 regulator. Mol. Microbiol. 82: 602–618.

McKinley, K. L., and I. M. Cheeseman, 2014 Polo-like kinase 1 licenses CENP-A deposition at centromeres. Cell 158: 397–411.

Measday, V., D. W. Hailey, I. Pot, S. A. Givan, K. M. Hyland *et al.*, 2002 Ctf3p, the Mis6 budding yeast homolog, interacts with Mcm22p and Mcm16p at the yeast outer kinetochore. Genes Dev. 16: 101–113.

Mitra, S., J. Gomez-Raja, G. Larriba, D. D. Dubey, and K. Sanyal, 2014 Rad51-Rad52 mediated maintenance of centromeric chromatin in Candida albicans. PLoS Genet. 10: e1004344.

Mukhopadhyay, A., B. Deplancke, A. J. Walhout, and H. A. Tissenbaum, 2008 Chromatin immunoprecipitation (ChIP) coupled to detection by quantitative real-time PCR to study transcription factor binding to DNA in Caenorhabditis elegans. Nat. Protoc. 3: 698–709.

Ortiz, J., O. Stemmann, S. Rank, and J. Lechner, 1999 A putative protein complex consisting of Ctf19, Mcm21, and Okp1 represents a missing link in the budding yeast kinetochore. Genes Dev. 13: 1140–1155.

Pascual-Ahuir, A., and M. Proft, 2007 Control of stress-regulated gene expression and longevity by the Sch9 protein kinase. Cell Cycle 6: 2445–2447.

Poddar, A., N. Roy, and P. Sinha, 1999 MCM21 and MCM22, two novel genes of the yeast Saccharomyces cerevisiae are required for chromosome transmission. Mol. Microbiol. 31: 349–360.

Roy, B., L. S. Burrack, M. A. Lone, J. Berman, and K. Sanyal, 2011 CaMtw1, a member of the evolutionarily conserved Mis12 kinetochore protein family, is required for efficient inner kinetochore assembly in the pathogenic yeast Candida albicans. Mol. Microbiol. 80: 14–32.

Sanyal, K., and J. Carbon, 2002 The CENP-A homolog CaCse4p in the pathogenic yeast Candida albicans is a centromere protein essential for chromosome transmission. Proc. Natl. Acad. Sci. USA 99: 12969–12974.

Sanyal, K., S. K. Ghosh, and P. Sinha, 1998 The MCM16 gene of the yeast Saccharomyces cerevisiae is required for chromosome segregation. Mol. Gen. Genet. 260: 242–250.

Sanyal, K., M. Baum, and J. Carbon, 2004 Centromeric DNA sequences in the pathogenic yeast Candida albicans are all different and unique. Proc. Natl. Acad. Sci. USA 101: 11374–11379.

Schaekel, A., P. R. Desai, and J. F. Ernst, 2013 Morphogenesis-regulated localization of protein kinase A to genomic sites in Candida albicans. BMC Genomics 14: 842.

Shang, C., T. R. Hazbun, I. M. Cheeseman, J. Aranda, S. Fields *et al.*, 2003 Kinetochore protein interactions and their regulation by the Aurora kinase Ipl1p. Mol. Biol. Cell 14: 3342–3355.

Stichternoth, C., A. Fraund, E. Setiadi, L. Giasson, A. Vecchiarelli *et al.*, 2011 Sch9 kinase integrates hypoxia and CO2 sensing to suppress hyphal morphogenesis in Candida albicans. Eukaryot. Cell 10: 502–511.

Thakur, J., and K. Sanyal, 2012 A coordinated interdependent protein circuitry stabilizes the kinetochore ensemble to protect CENP-A in the human pathogenic yeast Candida albicans. PLoS Genet. 8: e1002661.

Thakur, J., and K. Sanyal, 2013 Efficient neocentromere formation is suppressed by gene conversion to maintain centromere function at native physical chromosomal loci in Candida albicans. Genome Res. 23: 638–652.

Communicating editor: A. P. Mitchell

GENETICS

Supporting Information
http://www.genetics.org/lookup/suppl/doi:10.1534/genetics.114.173542/-/DC1

A Surprising Role for the Sch9 Protein Kinase in Chromosome Segregation in *Candida albicans*

Neha Varshney, Alida Schaekel, Rima Singha, Tanmoy Chakraborty, Lasse van Wijlick, Joachim F. Ernst, and Kaustuv Sanyal

DOI: 10.1534/genetics.114.173542

File S1

Strain construction

C. albicans strain AF1006 producing C-terminally HA-tagged Sch9 was constructed by transformation of heterozygous strain CAS2 by a tagging cassette generated by oligonucleotides Sch9-HA for/rev, as described (SCHAEKEL *et al.* 2013). Correct chromosomal integration was verified by colony PCR using primers Sch9ver and 3′ test HA-tag. Both alleles of *SCH9* were deleted in *C. albicans* strain RM1000AH (SANYAL *et al.* 2004) and 8675 (JOGLEKAR *et al.* 2008) using the URA blaster method. The construction of the URA blaster deletion cassette for *SCH9* was described previously (STICHTERNOTH *et al.* 2011). After the deletion of the first copy, the heterozygous strains were grown on 5-FOA plate to make the cells auxotroph for *URA3* to obtain RMKS1A, RMKS1B and 8675t. Then the same cassette was again used to disrupt the second allele of the gene, to get strains RMKS2A, RMKS2B and 8675T, respectively. To obtain the re-integrant of Sch9 in heterozygous and homozygous mutant background, the entire ORF along with its promoter and terminator was cloned in *Kpn*I and *Sal*I sites in CIp10 integration vector (MURAD *et al.* 2000). Sch9 orf was re-integrated at *RPS10* locus in the *Candida* genome using *Stu*I to obtain RMKS1AR, RMKS1BR, RMKS2AR and RMKS2BR. The correct chromosomal integration of CIp10 was verified by PCR using primers UP-RPS10 and NV207. To check the binding pattern of CENP-A across the centromere in *sch9* mutant by ChIP, one copy of CENP-A was tagged with Prot A using plasmid construct pCaCse4TAPNAT (THAKUR and SANYAL 2013). pCaCse4-TAP-NAT was partially digested with *Xho*I and transformed into RMKS2A to get Prot A tagged CENP-A strain.

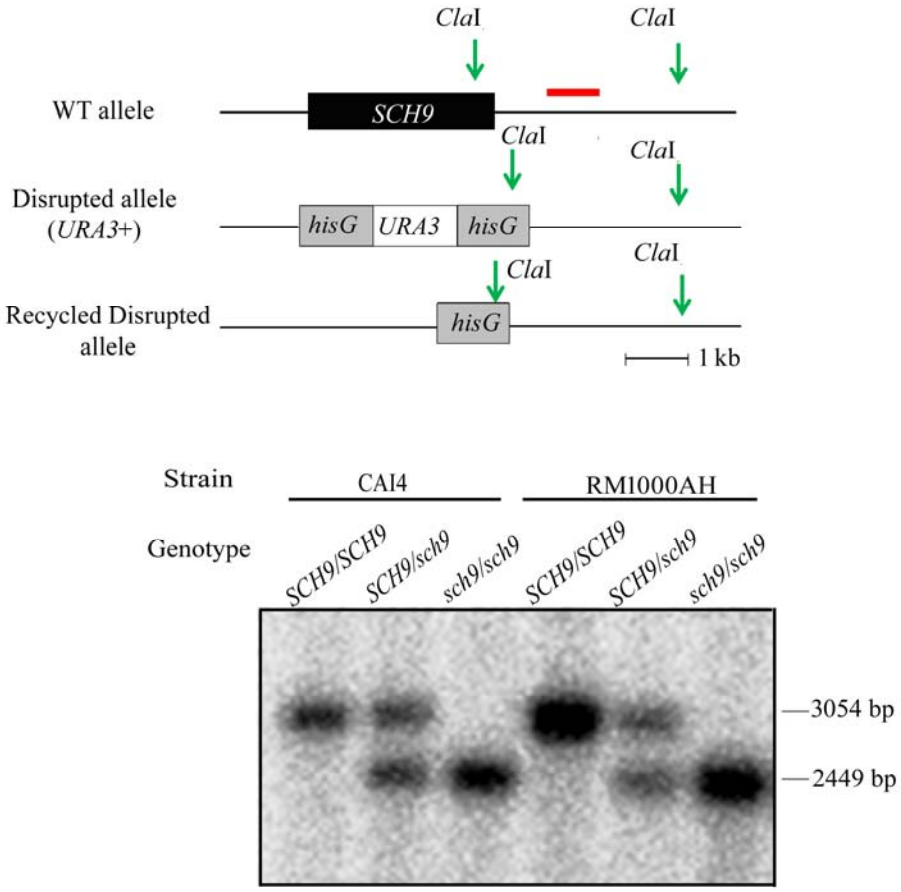

Figure S1 Southern blot analysis. Line diagrams showing wild-type and disrupted alleles of *SCH9*. *Cla*I digested DNA from wild-type strains (CAI4, RM1000AH) and corresponding heterozygous and null mutant strains lacking one or both copies of *SCH9* gene was separated on a agarose gel, blotted and probed with a region marked by the red line. Green arrows indicate *Cla*I sites. Bar, 1 kb.

	Percentage of cells with indicated morphology				Total no. of cells counted
					
CAI4	61.1	24.7	0.4	13.8	247
CAS1	69.1	24.7	0.7	6	133
CCS3	79.2	10.9	1.2	3.6	164

Figure S2 *C. albicans* wild-type (*SCH9/SCH9*), heterozygous (*SCH9/sch9*) and homozygous null mutant (*sch9/sch9*) strains were grown till OD_{600} ~ 1 at 30° in normoxic condition in YPDU and were stained with DAPI. A table showing percentages of cells with indicated morphologies of DAPI-stained nuclei.

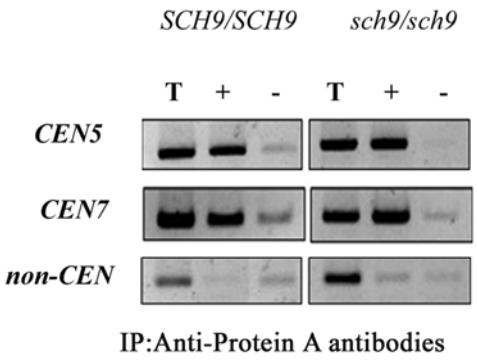

Figure S3 Cse4 localisation at the centromere is not affected by absence of Sch9. Standard ChIP assays were performed on strains CAKS102 (*CSE4-TAP/CSE4;SCH9/SCH9*) and J200T (*CSE4-TAP/Cse4; sch9/sch9*) (grown at 30°) using anti-Protein A (Cse4) antibodies. Enrichment at *CEN7*, *CEN5* and non-centromeric region was analysed using semi- quantitative PCR. PCR using total DNA (T) or ChIP DNA fractions with (+) or without (-) antibodies was performed.

Table S1 Strains used in this study

Name	Parent	Genotype	Reference
CAI4	SC5314	*ura3*::*imm434*/*ura3*::*imm434*	Fonzi *et al* 1993
CAS1	CAI4	as CAI4 but *SCH9/sch9::hisG-URA3-hisG*	Stichternoth *et al*, 2011
CAS2	CAS1	as CAI4 but *SCH9/sch9*::*hisG*	Stichternoth *et al*, 2011
CCS3	CAS2	as CAI4 but *sch9*::*hisG/sch9*::*hisG URA3/ura3*::*imm434*	Stichternoth *et al*, 2011
AF1006	CAS2	as CAS2 but *SCH9*::(*3xHA-URA3*)*/sch9*::*hisG*	This study
RM1000AH	RM1000	*Δura3*::*imm434/Δura3*::*imm434Δhis1*::*hisG/ Δhis1*::*hisG arg4*::*HIS1/ARG4*	Sanyal *et al*, 2004
RMKS1A	RM1000AH	*Δura3*::*imm434/ Δura3*::*imm434 Δhis1*::*hisG/ Δhis1*::*hisG arg4*::*HIS1/ARG4 sch9*::*hisG/SCH9*	This study
RMKS1B	RM1000AH	*Δura3*::*imm434/ Δura3*::*imm434 Δhis1*::*hisG/ Δhis1*::*hisG arg4*::*HIS1/ARG4 sch9*::*hisG/SCH9*	This study
RMKS2A	RMKS1A	*Δura3*::*imm434/ Δura3*::*imm434 Δhis1*::*hisG/ Δhis1*::*hisG arg4*::*HIS1/ARG4 sch9*::*hisG/sch9*::*hisG-URA3-hisG*	This study
RMKS2B	RMKS1B	*Δura3*::*imm434/ Δura3*::*imm434 Δhis1*::*hisG/ Δhis1*::*hisG arg4*::*HIS1/ARG4 sch9*::*hisG/sch9*::*hisG-URA3-hisG*	This study
RMKS1AR	RMKS1A	*Δura3*::*imm434/ Δura3*::*imm434 Δhis1*::*hisG/ Δhis1*::*hisG arg4*::*HIS1/ARG4 sch9*::*hisG/SCH9/Cip10-SCH9*	This study
RMKS1BR	RMKS1B	*Δura3*::*imm434/ Δura3*::*imm434 Δhis1*::*hisG/ Δhis1*::*hisG arg4*::*HIS1/ARG4 sch9*::*hisG/SCH9/ Cip10-SCH9*	This study
RMKS2AR	RMKS2A	*Δura3*::*imm434/ Δura3*::*imm434 Δhis1*::*hisG/ Δhis1*::*hisG arg4*::*HIS1/ARG4 sch9*::*hisG/sch9*::*hisG-URA3-hisG/ Cip10-SCH9*	This study
RMKS2BR	RMKS2B	*Δura3*::*imm434/ Δura3*::*imm434 Δhis1*::*hisG/ Δhis1*::*hisG arg4*::*HIS1/ARG4 sch9*::*hisG/sch9*::*hisG-URA3-hisG/ Cip10-SCH9*	This study
8675	BWP17	*Δ ura3*::*λimm434/ Δ ura3*::*imm434 Δhis1*::*hisG/Δhis1*::*hisGΔarg4*::*hisG/arg4*::*hisG CSE4/CSE4:GFP:CSE4*	Joglekar*et al*, 2008

8675t	8675	*Δ ura3::λimm434/Δura3::imm434 Δhis1::hisG/Δhis1::hisGΔarg4::hisG/Δarg4:: hisG CSE4/CSE4:GFP:CSE4 sch9::hisG/SCH9*	This study
8675T	8675t	*Δ ura3::λimm434/Δura3::imm434 Δhis1::hisG/Δhis1::hisGΔarg4::hisG/Δarg4:: hisG CSE4/CSE4:GFP:CSE4 sch9::hisG/sch9::hisG-URA3-hisG*	This study
CAKS102	SN148	*Δura3::imm434/Δura3::imm434, Δhis1::hisG/Δhis1::hisG, Δarg4::hisG/Δarg4::hisG, Δleu2::hisG/Δleu2::hisG CSE4/CSE4-TAP(URA3)*	Mitra *et al*, 2014
J200	RM1000AH	*Δura3::imm434/ Δura3::imm434 Δhis1::hisG/ Δhis1::hisG arg4::HIS1/ARG4 CSE4/CSE4TAP-NAT*	Thakur *et al*, 2013
J200T	J200	*ura3::imm434/ ura3::imm434 his1::hisG/his1::hisG arg4::HIS1/ARG4 sch9::hisG/sch9::hisG-URA3-hisG CSE4::CSE4-TAP-NAT*	This study

Table S2 Primers used in this study

Primer name	Sequence	Description
2498-21	CTG GTG CAA GAC CCT CAT AGA AGC	Semi-quantitative ChIP PCR primers for CEN7
2498-22	CCT GAC ACT GTC GTT TCC CAT AGC	Semi-quantitative ChIP PCR primers for CEN7
CEN5e	TGTTCTGACATACTGGGTAGACTTT	Semi-quantitative ChIP PCR primers for CEN5
CEN5f	CGAAGCATTTTGTATAACAGCCC	Semi-quantitative ChIP PCR primers for CEN5
CACH5R1	TTCATGGAAGAGGGGTTTCA	qPCR primers for CEN5
CACH5F1	CCCGCAAATAAGCAAACACT	qPCR primers for CEN5
NCEN7-3	GCATACCTGACACTGTCGTT	qPCR primers for CEN7
NCEN7-4	AACGGTGCTACGTTTTTTTA	qPCR primers for CEN7
Ctrl 7 a	ACTCGCCTTCCCCTCCTTTAAATAG	qPCR and semi-quantitative ChIP PCR primers for non centromeric region
Ctrl 7 b	CCACTACTACGACTGTGGATTCACT	qPCR and semi-quantitative ChIP PCR primers for non centromeric region
Sch9-HA for	GAAGAAGAAGATGAAATGGAAGTTGATGAAGAT CAACATATGGATGATGAATTTGTCAATGGAAGAT TTGATCTTGGTGGTGGTCGGATCCCCGGGTTAAT TAA	HA tagging
Sch9-HA rev	GCACAAAATGGAGAAGGAGAAAAAGTAGGAAC GGAATTCTATTGAATGGAACAGTTTAGTTCTAGA AGGACCACCTTTGATTG	HA tagging
Sch9ver	GTTGATTTCTGGTCATTAGG	Tagging verification primers
3‘ test HA-tag	CATCGTATGGGTAAAAGATG	Tagging verification primers
NV195	AGTGGTACCGGTCGATGTATAACTTCATTTCAT	CIp10 cloning forward
NV196	ACGCGTCGAGCAC AGA CAT TGG GCA AGA AA	CIp10 cloning reverse
UP-RPS10	TTCTGGTGTTCTCTCACTGTTAAGC	CIp10 integration confirmation forward
NV207	GAGTTATTAGCCCTGCGATCTTTG	CIp10 integration confirmation reverse

Literature Cited

JOGLEKAR, A. P., D. BOUCK, K. FINLEY, X. LIU, Y. WAN *et al.*, 2008 Molecular architecture of the kinetochore-microtubule attachment site is conserved between point and regional centromeres. J Cell Biol **181:** 587-594.

MURAD, A. M., P. R. LEE, I. D. BROADBENT, C. J. BARELLE and A. J. BROWN, 2000 CIp10, an efficient and convenient integrating vector for Candida albicans. Yeast **16:** 325-327.

SANYAL, K., M. BAUM and J. CARBON, 2004 Centromeric DNA sequences in the pathogenic yeast Candida albicans are all different and unique. Proc Natl Acad Sci U S A **101:** 11374-11379.

SCHAEKEL, A., P. R. DESAI and J. F. ERNST, 2013 Morphogenesis-regulated localization of protein kinase A to genomic sites in Candida albicans. BMC Genomics **14:** 842.

STICHTERNOTH, C., A. FRAUND, E. SETIADI, L. GIASSON, A. VECCHIARELLI *et al.*, 2011 Sch9 kinase integrates hypoxia and CO2 sensing to suppress hyphal morphogenesis in Candida albicans. Eukaryot Cell **10:** 502-511.

THAKUR, J., and K. SANYAL, 2013 Efficient neocentromere formation is suppressed by gene conversion to maintain centromere function at native physical chromosomal loci in Candida albicans. Genome Res **23:** 638-652.